

# Sulfur Differentiation in Organic-Rich Shales and Carbonates via Open-System Programmed Pyrolysis and Oxidation: Insights into Fluid Sourcing and H<sub>2</sub>S Production in the Bakken Shale, United States

Humberto Carvajal-Ortiz, Thomas Gentzis,\* and Mehdi Ostadhassan

Cite This: <https://doi.org/10.1021/acs.energyfuels.1c01562>

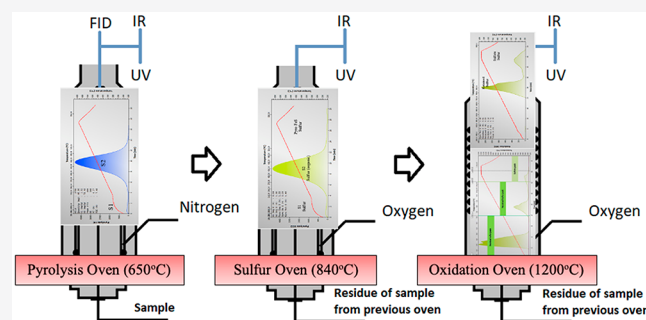
Read Online

ACCESS |

Metrics & More

Article Recommendations

**ABSTRACT:** The amount of organic sulfur influences the kinetic behavior of kerogen upon thermal maturation as well as the crude quality and sourness. There has always been an interest to specify the amount and different forms of sulfur in source and reservoir rocks. In this study, we analyzed 28 samples from the Bakken Formation having different maturities and 5 samples from other shales containing type I, type IS, or type IIS kerogen using the Rock-Eval 7S instrument. Total sulfur data were compared to those from LECO SC-632 and CHNS elemental analyzer, with excellent to very good correlation, respectively. The sulfur index is a fast and reliable method to differentiate between type I and type II kerogens against their S-rich counterparts. Organic sulfur in the Bakken is not massively associated with S<sub>2</sub> but with the refractory component of total organic carbon (S<sub>4</sub>). Thus, not all total organic sulfur (TOS) is responsible for the early generation of liquid hydrocarbons in organic-rich shales. Also, TOS should not be used as an indicator of kerogens being “type S”. Residual S<sub>org</sub> in the Bakken increased with maturity, and a considerable amount was available to generate H<sub>2</sub>S at relatively low temperatures via aquathermolysis, a process that occurs in the Greater Permian Basin. High concentrations of residual TOS in the Bakken (average of 2.3 wt % on whole-rock basis) meet the minimum of 1.4 wt % S (on a kerogen basis) required for H<sub>2</sub>S production. This suggests a possible correlation between TOS and high H<sub>2</sub>S production in Williston and other basins.



## 1. INTRODUCTION

The accumulation and preservation of organic matter (OM) in sedimentary basins and their fate as a fraction of the weight percent of sedimentary rocks are concepts accepted and commonly used by many geoscientists (i.e., sedimentologists, petrographers, and geochemists). The preferential preservation of relatively large quantities of OM in sedimentary rocks often leads to the formation of organic-rich intervals, commonly known as petroleum source rocks.<sup>1</sup> A petroleum source rock (or simply “source rock”) is arguably the most important element in both conventional and unconventional petroleum systems. For the latter, having a good source reservoir is a must have trait to every liquid-rich or gas shale unconventional play.<sup>2</sup>

In many depositional environments, the preservation of OM is enhanced (or shielded from recycling and dilution) by many factors, with one of those being the sulfurization or vulcanization of sedimentary OM. The vulcanization of OM during diagenesis occurs when lipids preferentially incorporate sulfur into their chemical structure, producing kerogen moieties that are more recalcitrant to recycling, specially under oxygen-limiting conditions.<sup>3–5</sup>

Vulcanization of OM ultimately generates kerogens that are enriched in organic sulfur. Such kerogens (commonly referred to as type IIS and type IS kerogens) tend to be more reactive (labile) than their more sulfur-lean counterparts (type II and type I kerogens).<sup>6</sup> When experiencing thermal stress (i.e., as thermal maturity increases), type IIS and type IS kerogens generate hydrocarbons in economic quantities at lower levels of thermal maturity (e.g., vitrinite reflectance of <0.6% or  $T_{\max}$  of <430 °C) than expected.<sup>4,7–9</sup> Once vulcanization of OM has occurred, sulfur chemistry influences the response of kerogen to increasing thermal stress, something that has critical implications for basin modeling, timing of oil generation and expulsion, and oil quality.<sup>9–14</sup>

Understanding sulfur geochemistry in sedimentary basins has also become an important safety and environmental factor

Received: May 20, 2021

Revised: June 22, 2021

when designing conventional and unconventional extraction strategies (e.g., steam injection and hydraulic fracturing) as a result of the potential of these recovery techniques to generate hazardous and toxic hydrogen sulfide gas ( $\text{H}_2\text{S}$ ). The presence of  $\text{H}_2\text{S}$  at concentrations of  $>100$  ppm (classifying a gas as  $\text{H}_2\text{S}$ -rich) increases the cost of oil and gas exploration, development, and production. For instance,  $\text{H}_2\text{S}$  generation associated with bitumen or heavy oil production by steam injection is a major concern for operations in many areas, such as Athabasca (Canada) and Venezuela, where the increase in steam-assisted gravity drainage (SAGD) programs occurs in parallel with rising of  $\text{H}_2\text{S}$  levels as wells age.<sup>15</sup>  $\text{H}_2\text{S}$  generation in the reservoir during SAGD is caused by aquathermolysis reactions of bitumen or heavy oil together with the rock matrix. These reactions transform some sulfur-containing compounds (typically kerogen bound) into  $\text{H}_2\text{S}$ .<sup>15,16</sup> Similarly, across the Greater Permian Basin in West Texas and New Mexico, U.S.A., close to 85% of the gas in wells is  $\text{H}_2\text{S}$ -rich ( $>100$  ppm), and more than 40% of the gas streams have  $\text{H}_2\text{S}$  of  $>10\,000$  ppm.<sup>17,18</sup>

Despite the important role that sulfur geochemistry plays in understanding both the thermal evolution of source rocks [especially in the context of liquid-rich unconventional (LRU) plays] and the presence of  $\text{H}_2\text{S}$ -rich gas during conventional and unconventional operations, very few studies have attempted to investigate the consequences of having sulfur-rich OM in mature or underexplored basins.<sup>4,10–12,14,17,18</sup> Moreover, to this day, little is still known about the amount and forms of sulfur in most kerogens.<sup>19,20</sup> Even total organic sulfur in kerogens [ $\text{TOS} = \text{S1-S} + (\text{S2} - \text{S4})\text{S}$ ] is not routinely determined, mainly because of common contamination by pyrite that makes the analysis and interpretations derived from it challenging.<sup>7,10</sup> The main reason for this lies in the technical challenges to separate organic from inorganic sulfur moieties prior to analysis. Conventional ways of separating organic from inorganic sulfur rely heavily on wet chemistry procedures. Wet chemistry separation of sulfur fractions in sedimentary rocks is time-consuming and labor-intensive and requires the use of dangerous reagents (e.g., zinc bromide, acidic chromium chloride, nitric acid, etc.). For instance, nitric acid has been routinely used since the late 1980 and early 1990 studies.<sup>8,19</sup> It is common to read in the literature that, to account for incomplete removal of pyrite, samples are simply treated for kerogen concentration (removal of carbonates and silicates via  $\text{HCl}$  and  $\text{HF}$ ), and then the iron content in kerogen is used to estimate the amount of pyrite-associated sulfur in the kerogen, assuming that all iron in the isolated kerogen was in the pyrite [confirmed by X-ray diffraction (XRD) analyses]. This way, the measured total sulfur in the kerogen is corrected for the estimated pyritic sulfur to calculate the organic sulfur content.<sup>8,14,20</sup> However, all of these wet-chemistry-based techniques are cumbersome and often not totally satisfactory.<sup>10</sup>

Alternative methods exist to overcome the pyrite contamination problem occurring with wet chemistry. Sulfur speciation can be performed using K-edge X-ray absorption near-edge structure (XANES) spectroscopy.<sup>18–26</sup> XANES can provide information on the distribution of different ways sulfur bonds in kerogen (oxidation states).<sup>27</sup> However, obtaining accurate XANES spectra for sulfur speciation is not an easy task because the proximity of the sulfide and thiophene peaks introduces a significant uncertainty to the results.<sup>24</sup> Moreover, XANES does not provide total sulfur concentrations for each fraction, and sulfur contents [total sulfur ( $\text{TS}$ ) =  $\text{TOS}$  +

(inorganic S),  $\text{TOS}$ , pyritic sulfur, etc.] are still measured by traditional wet chemistry separation with combustion-based elemental analysis.<sup>14,20</sup>

Although XANES and other sophisticated analytical tools can provide partial answers to the problem, sulfur can also be studied by customizing oxidation and pyrolysis ovens. Pioneering experiments in this area were performed by Madec and Espitalié,<sup>28</sup> where organic sulfur was differentiated from pyritic sulfur (i.e., present in sulfides like pyrite) through programmed pyrolysis in a customized Rock-Eval apparatus. However, this instrument was not equipped with a second oven for oxidation (i.e., both pyrolysis and oxidation were performed in the same oven, which is a major flaw in the design of some pyrolyzers). The systematic errors and discrepancies observed with single-oven instruments occur because pyrolysis and oxidation processes occurred in the same oven. A hysteresis phenomenon is observed after testing organic-rich and organic-poor samples back to back. The observed  $\text{S}_4\text{CO}_2$  and  $\text{S}_4\text{CO}$  peaks that evolve in organic-poor samples are usually many times greater when the sample is analyzed in single-oven analyzers. This phenomenon does not occur when the same set of samples are analyzed in instruments with two ovens (separate pyrolysis and oxidation processes). Hysteresis can be explained by the fact that, in single-oven designs, hydrocarbon solids are being deposited in the tubing connecting the oven to the infrared (IR) cell. During the oxidation stage, these deposits are oxidized into  $\text{CO}_2$ , thereby yielding an incorrect reading for  $\text{S}_4\text{CO}_2$  [part of the residual organic carbon (ROC)], by generating  $\text{S}_4\text{CO}_2$  many times greater than the real value.

In the present study, we have analyzed 28 samples from 9 wells from the Upper and Lower members of the Bakken Shale Formation (UBS and LBS, respectively) across the Williston Basin, North Dakota, using a new Rock-Eval analyzer model, denominated Rock-Eval 7S (Vinci Technologies and IFFen methods). The Rock-Eval 7S performs “live” separation and quantification of sulfur yields coming from organic and inorganic moieties (measured as  $\text{SO}_2$  during pyrolysis and oxidation, in addition to hydrocarbon,  $\text{CO}$ , and  $\text{CO}_2$  detection).<sup>29–31</sup> We have also analyzed additional samples from formations containing type IS (organic-rich carbonate facies of Kimmeridgian age) and type IIS (Monterey Shale from U.S.A., Kimmeridge Clay from the U.K., and Pantokrator Shale from western Greece) kerogens and compared their organic sulfur content to that of the UBS and LBS samples.

The UBS and LBS samples selected cover the maturity spectrum for oil generation (from immature to late oil window). This was necessary to understand the reasons for the high volumes of  $\text{H}_2\text{S}$  production in specific regions/wells in the Williston Basin. The souring of oil from reservoirs in the Bakken Formation has been observed in the field.<sup>32</sup> In addition to the environmental implications, sour oil and gas have a much lower profit margin ( $\sim 10\%$  lower price) than traditional sweet Bakken crude oil.<sup>32,33</sup> The present study focused on the recorded evidence of  $\text{H}_2\text{S}$  production or shows in some of the 28 wells analyzed and investigated the possibility of bulk organic geochemical factors (i.e., organic sulfur content) as key drivers for the origination of sour gas in the Bakken Shale. This study shows a fast, safe, and inexpensive alternative for organic sulfur detection and quantification to methods, such as XANES, atomic analyses, and X-ray photoelectron spectroscopy (XPS), particularly in situations where the presence of

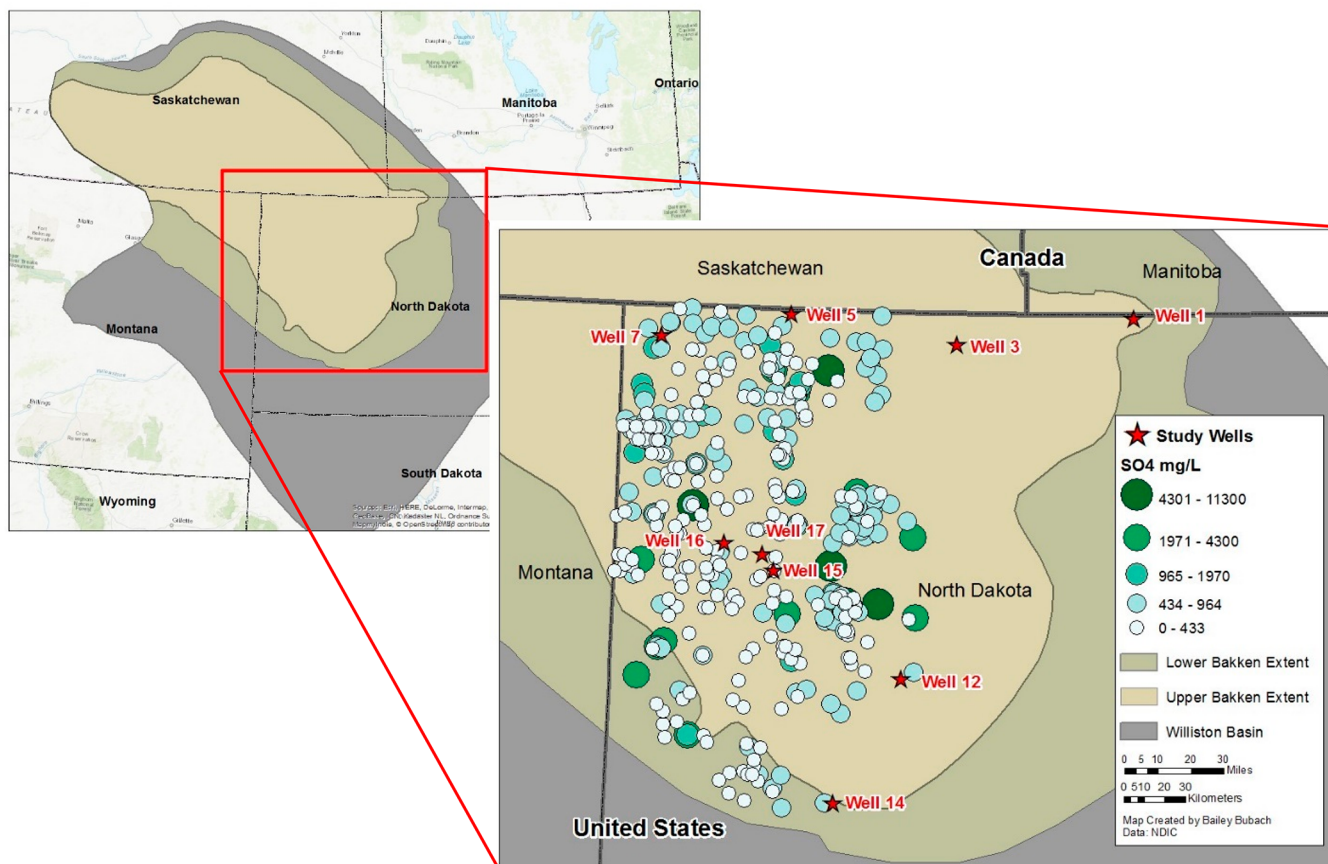


**Figure 1.** Geographical location of the Bakken Formation and studied wells (red stars). Values of measured  $\text{SO}_4$  at well locations through the drill stem test are also shown (map is courtesy of Bailey Bubach, University of North Dakota).

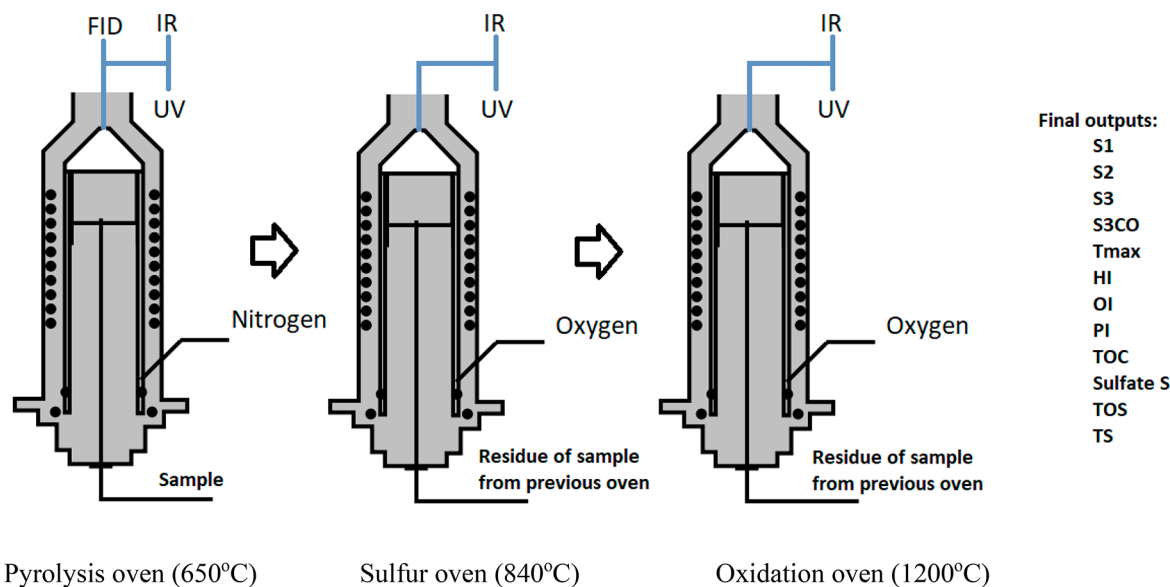


**Figure 2.** Schematic of Rock-Eval 7S including three ovens for sulfur speciation. The output also includes the sulfur index (SI).

$\text{H}_2\text{S}$  seems to be problematic, and thus, a proper sulfur geochemistry assessment is mandatory.

**2. SAMPLES AND METHODS**

**2.1. Sample Selection.** The 28 samples of the Bakken Formation from 9 wells were carefully selected to cover areas with both UBS and LBS showing different thermal maturities. Figure 1 shows well

locations (red stars) and the amount of sulfate ( $\text{SO}_4$ ) detected across the Williston Basin in North Dakota.

Additional samples were selected from thermally immature outcrops of the Upper Jurassic Kimmeridge Clay Formation in the U.K., the Eocene Green River Shale Formation in the U.S.A., organic-rich carbonate facies of Kimmeridgian age (Orbagnoux Carbonates, France), the Miocene Monterey Shale in the U.S.A., and the Jurassic Pantokrator Shale from Greece. The Kimmeridge Clay sample was



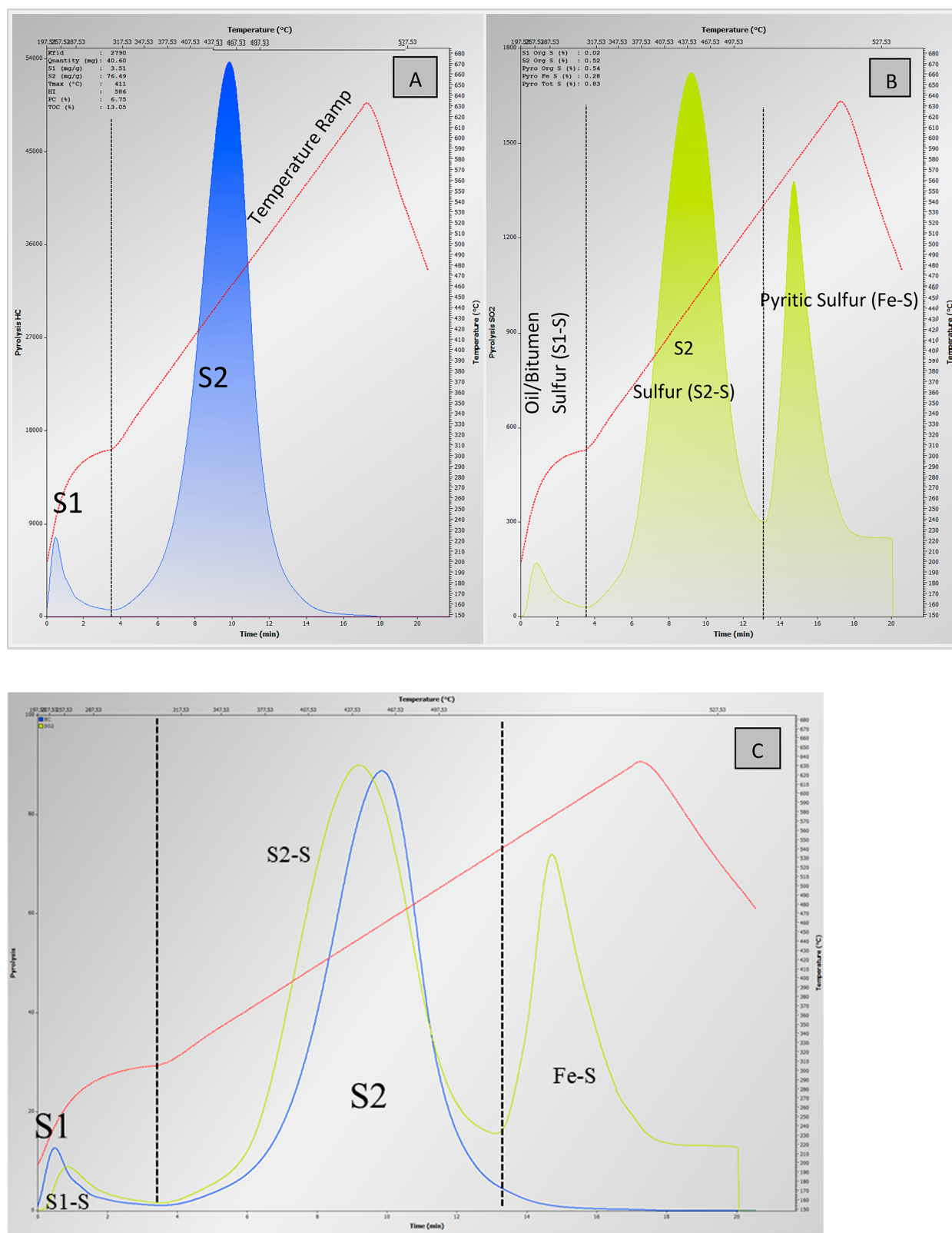


**Figure 3.** (A) Pyrogram of an Upper Bakken Shale sample from well 17, (B) sulfur pyrogram of the same sample, and (C) superimposed FID (hydrocarbons) and UV (sulfur) pyrograms.

collected from an outcrop in the type area on the Dorset coast of England. Organic facies of the Kimmeridge Clay in the Dorset area are known for their high organic sulfur content, reaching the type IIS status in some areas.<sup>4</sup> The Green River Shale sample is from the Mahogany zone and was collected from an outcrop at the Anvil Points

Mine, Piceance Basin, Colorado. The Green River shale sample is used here as an endmember of type I OM (and the most organic sulfur lean).

The Monterey Formation sample was collected at Lions Head, Santa Maria Basin (California, U.S.A.). The Monterey Formation at

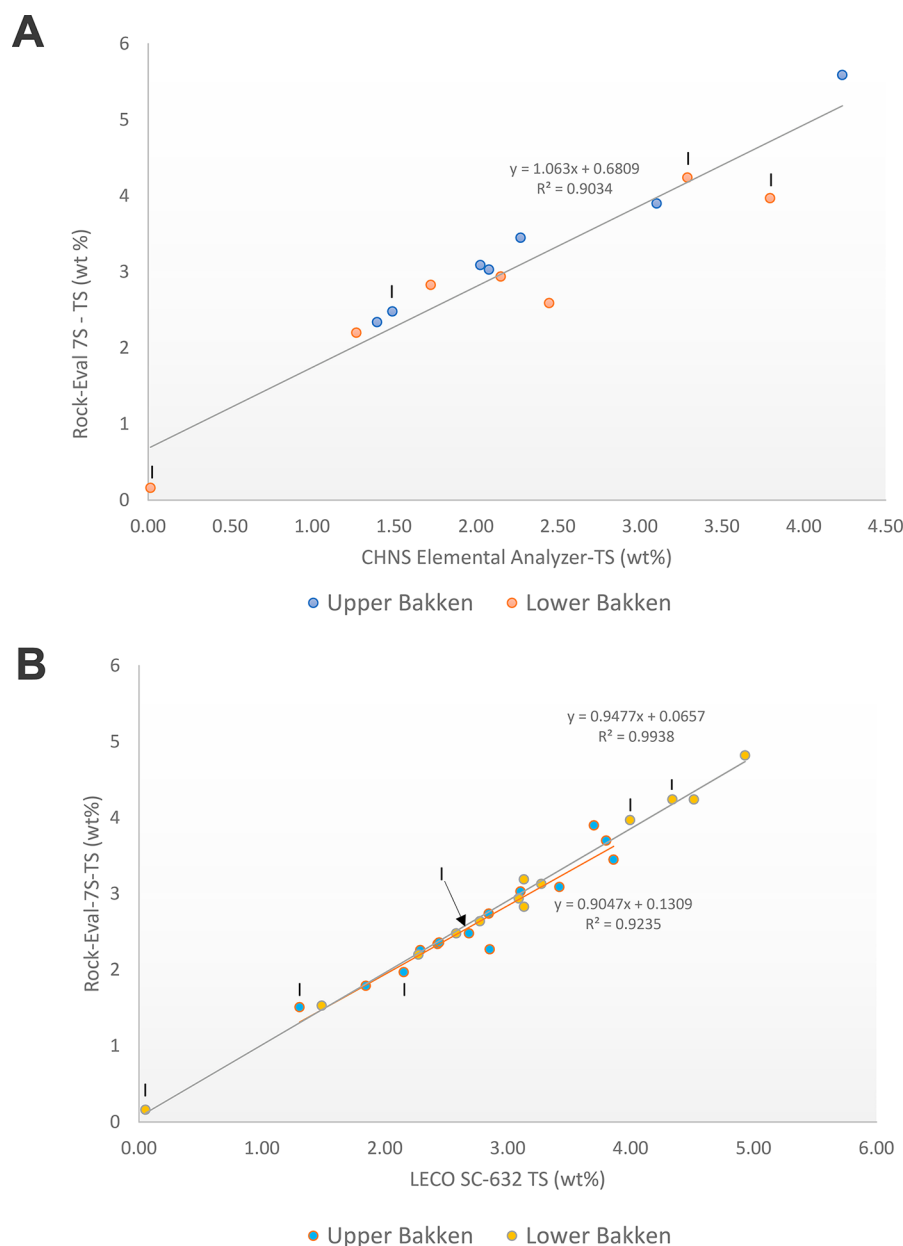


**Figure 4.** (A) TS from the CHNS analyzer versus TS from Rock-Eval 7S presenting a good correlation between the results from both techniques. I = immature samples (<435 °C). Not all immature samples were analyzed by the elemental analyzer. All other samples in the figure are mature. (B) Comparison of TS derived from a LECO SC-632 analyzer and Rock-Eval 7S. Notice the excellent correlation between the two techniques (similar combustion temperatures and “live” detection). I = immature samples (<435 °C). All 28 samples were analyzed by LECO. All other samples in the figure without the symbol “I” are mature.

this location is characterized as type IIS kerogen but with relative lower organic sulfur content than the Monterey Formation from Naples Beach (Santa Barbara-Ventura Basin, California, U.S.A.).<sup>11</sup> The organic sulfur content ( $S_{\text{org}}$ ) at this location is comparable to the highest  $S_{\text{org}}$  contents reported for the Kimmeridge Clay from the Dorset coast of England.<sup>4</sup> The type IS sample (Orbagnoux Carbonates, France) was provided by the IFPen, and samples from this locality are used routinely as calibration and check standards during Rock-Eval 7S sulfur runs. The Pantokrator Shale sample from Greece was provided by Dr. Ioannis Oikonomopoulos (Hellenic Petroleum). The sample was collected off the Ionian zone in western Greece.

**2.2. Organic Sulfur Quantification via Open-System Programmed Pyrolysis and Oxidation.** About 50 mg of crushed material were analyzed using a Rock-Eval 7S analyzer (Vinci Technologies, France).<sup>31</sup> The Rock-Eval 7S was used because of its

sulfur detection capabilities and ability to directly quantify the TOS in whole-rock and kerogen concentrate samples. The amount of organic sulfur in sedimentary OM (quantified as TOS) is a critical parameter that directly influences source-rock kinetics and, thus, thermal conversion of OM into hydrocarbons. The sulfur speciation analysis was performed using the basic/total sulfur method (IFPen methods). The temperature program is similar to the basic/bulk-rock method widely used in the industry (pyrolysis isothermal at 300 °C for 3 min, followed by a 25 °C/min ramp until 652 °C,<sup>34</sup> but with an extra oven step during the pyrolysis stage (the sulfur oven where the evolved gases are oxidized into  $\text{SO}_2$  at 840 °C) and an extended analysis time during the oxidation stage (with a 20 °C/min ramp from 300 to 1200 °C for full decomposition of sulfate moieties).  $\text{SO}_2$  released during both pyrolysis and oxidation is measured in real time by an ultraviolet (UV) detector. In addition to detection of TS and TOS, the instrument is capable of separating and quantifying pyritic sulfur (Fe-

Table 1. (a) Source-Rock Parameters for 28 Bakken Shale Samples and 5 Outcrop Samples from Various Formations and (b) Top of the Upper and the Lower Bakken Formation in the Wells Used in This Study<sup>a</sup>

**a**

Sample No.	Well	Fm.	Depth (ft)	S1 (mg/g)	S2 (mg/g)	Tmax (°C)	TOC (wt. %)	EA-TS	LECO-TS	RE7-TS
BK13	12	U.B	9444.5	6.91	104.18	430	16.26	1.49	2.69	2.48
BK3	3	U.B	5996	6.05	89.16	431	17.21		1.31	1.51
BK14	12	U.B	9450.5	7.72	84.39	434	23.44		2.15	1.97
BK18	14	U.B	9672.2	5.35	72.99	435	13.41	2.08	3.11	3.03
BK9	7	U.B	8205.2	5.14	101.47	436	17.8		4.21	4.05
BK10	7	U.B	8200.7	4.22	63.07	438	14.56	2.27	3.86	3.45
BK17	14	U.B	9669	5.83	82.82	438	11.88		2.85	2.74
BK5	5	U.B	7344.9	6.28	122.5	439	12.95	4.4	5.21	5.59
BK6	5	U.B	7335.5	3.19	70.24	444	14.45		2.29	2.26
BK21	16	U.B	11272	11.55	13.26	449	8.54	1.4	2.43	2.34
BK20	15	U.B	10758	5.89	19.43	450	13.57		2.85	2.27
BK19	15	U.B	10755	5.83	20.54	451	12.75	3.1	3.7	3.9
BK22	16	U.B	11261	10.05	19.48	454	12.84		2.69	3.47
BK26	17	U.B	10868	11.96	16.38	458	11.58		2.44	2.36
BK25	17	U.B	10858	5.67	18.87	465	10.25	2.03	3.42	3.09
BK1	1	L.B	3783	3.37	61.29	416	11.19		4.52	4.24
BK2	1	L.B	3780	3.51	76.49	417	13.05	3.8	4	3.97
BK4	3	L.B	6021.5	0.26	0.79	425	2.44	0.02	0.05	0.06
BK15	12	L.B	9508	7.94	119.82	425	21.82	3.29	4.34	4.24
BK16	12	L.B	9504	6.49	91.38	432	15.8		3.27	3.13
BK11	7	L.B	8285.5	6.85	81.68	436	16.73	2.15	3.09	2.94
BK12	7	L.B	8272	3.85	72.66	438	11.68		3.13	3.19
BK7	5	L.B	7425	7.89	87.25	441	15.24		4.5	3.74
BK8	5	L.B	7434.5	4.3	59.6	442	13.31	2.45		2.59
BK27	17	L.B	10921	8.64	18.89	457	11.72		1.49	1.53
BK24	16	L.B	11331	6.98	18.33	457	12.39		2.77	2.64
BK28	17	L.B	10931	5.8	19.17	458	14.27	1.27	2.27	2.2
BK23	16	L.B	11322	6.01	13.23	460	14.41	1.72	3.13	2.83
KC	-	Kimm. Clay	Outcrop	1.43	255.79	418	36.69			5.6
GR	-	Green River	Outcrop	1.24	180.72	440	19.63			0.83
TI-S	-	Orbagnoux	Outcrop	1.69	68.25	412	7.11			2.39
Monterey	-	Monterey	Outcrop	1.29	47.27	406	6.19			2.16
Pantokrator	-	Pantokrator	Outcrop	2.33	219.08	415	28.4			5.77

**b**

Well	Top U.B (TVD-ft)	Top L.B (TVD-ft)
1	3694	3746
3	6043	6064
5	7327	7404
7	8198	8268
12	9440	9500
14	9700	9720
15	10750	10802
16	11258	11313
17	10854	10917

<sup>a</sup>TVD = true vertical depth.

S), bitumen/oil organic sulfur (S1-S), organic sulfur associated with hydrocarbon prone kerogen (S2-S), and organic sulfur associated with oxidized OM (ROS or S4-S). The process considers the pyrite thermal degradation rate, impact of the mineral matrix, and impact of the organic matrix.<sup>31</sup> More details of the sulfur speciation using Rock-Eval 7S instrumentation can be found in the studies of Wattripont et al.<sup>29</sup> and Aboussou et al.<sup>30,31</sup> Figure 2 shows a schematic of the instrumentation. Panels A–C of Figure 3 show the pyrogram of an UBS sample from well 17 showing the separation between S1-S, S2-S, and Fe-S.

### 2.3. Elemental CHNS and Combustion (LECO) Analyses.

Some of the Bakken Shale samples analyzed by Rock-Eval 7S TS were also analyzed by both an elemental CHNS analyzer (14 samples from the UBS and 14 samples from the LBS) and a LECO SC-632 analyzer (all 28 Bakken Shale samples) to cross-check the accuracy of the results for TS quantification.

A CHNS elemental analyzer provides the means for a rapid determination of carbon, hydrogen, nitrogen and sulfur in organic matrices and other types of materials.<sup>35</sup> About 2–5 mg of the sample is introduced into a dynamic flash combustion. In the combustion process (furnace at approximately 1000 °C), carbon is converted to carbon dioxide, hydrogen is converted to water, nitrogen is converted to nitrogen gas/oxides of nitrogen, and sulfur is converted to sulfur dioxide. The combustion products are swept out of the combustion chamber by an inert carrier and then passed over heated copper (about 600 °C). The gases are then passed through the absorbent traps to leave only carbon dioxide, water, nitrogen, and sulfur dioxide.<sup>36</sup> Combustion analyses on the same samples were conducted using a LECO SC-632 model, where the sample is crushed, loaded into a ceramic crucible, and combusted at 1350 °C. Live detection of evolved SO<sub>2</sub> was performed via an IR cell. The results from both comparisons are shown in panels A and B of Figure 4 and Table 1a.

**Table 2. Key Sulfur Parameters Detected via Rock-Eval 7S Pyrolysis and Oxidation Analyses for 28 Bakken Shale Samples and 5 Outcrop Samples from Various Formations<sup>a</sup>**

Sample No.	Well	Fm.	Depth (ft)	TS (wt%)	TOS (wt%)	S2-S (wt%)	HI (mgHC/gTOC)	SI (mg Sorg/gTOC)
BK13	12	U.B	9444.5	2.48	1.86	0.37	641	21
BK3	3	U.B	5996	1.51	1.11	0.23	518	14
BK14	12	U.B	9450.5	1.97	1.29	0.3	360	22
BK18	14	U.B	9672.2	3.03	1.95	0.28	544	22
BK9	7	U.B	8205.2	4.05	2.9	0.4	570	22
BK10	7	U.B	8200.7	3.45	1.82	0.23	433	19
BK17	14	U.B	9669	2.74	1.83	0.31	697	21
BK5	5	U.B	7344.9	5.59	3.52	0.42	946	18
BK6	5	U.B	7335.5	2.26	1.77	0.21	486	15
BK21	16	U.B	11272	2.34	1.19	0.03	155	4
BK20	15	U.B	10758	2.27	1.48	0.05	143	4
BK19	15	U.B	10755	3.9	2.4	0.09	161	7
BK22	16	U.B	11261	3.47	2.65	0.03	152	2
BK26	17	U.B	10868	2.36	1.47	0.03	141	3
BK25	17	U.B	10858	3.09	2.16	0.06	184	5
BK1	1	L.B	3783	4.24	3.1	0.42	548	38
BK2	1	L.B	3780	3.97	2.95	0.52	586	40
BK4	3	L.B	6021.5	0.16	0.11	0.02	32	8
BK15	12	L.B	9508	4.24	2.63	0.46	549	21
BK16	12	L.B	9504	3.13	2.14	0.32	578	20
BK11	7	L.B	8285.5	2.94	2.16	0.31	488	20
BK12	7	L.B	8272	3.19	2.15	0.31	622	23
BK7	5	L.B	7425	3.74	1.73	0.35	573	21
BK8	5	L.B	7434.5	2.59	1.5	0.21	448	18
BK27	17	L.B	10921	1.53	1.05	0.03	161	2
BK24	16	L.B	11331	2.64	2.14	0.03	148	2
BK28	17	L.B	10931	2.2	1.55	0.05	134	4
BK23	16	L.B	11322	2.83	1.57	0.05	92	4
KC	-	Kimm. Clay	Outcrop	5.60	5.25	4.06	697	111
GR	-	Green River	Outcrop	0.83	0.72	0.22	921	11
TI-S	-	Orbagnoux	Outcrop	2.39	2.05	1.53	960	215
Monterey	-	Monterey	Outcrop	2.16	1.67	1.02	764	165
Pantokrator	-	Pantokrator	Outcrop	5.77	4.62	3.84	771	135

<sup>a</sup>TS, total sulfur; TOS, total organic sulfur; S2-S, reactive organic sulfur associated with the pyrolysis S2 parameter; HI, hydrogen index; and SI, sulfur index.

The depths to the top of the Lower and Upper Bakken Formation in the wells used in this study are shown in Table 1b. The Rock-Eval 7S TS results are in good agreement with the CHNS elemental analyzer results and in excellent agreement with the LECO SC-632 results.

Minor discrepancies can be observed between the CHNS elemental analyzer results and both LECO combustion and Rock-Eval 7S results. The elemental analyzer does not seem to fully decompose sulfur species (especially sulfates), only reaching 1000 °C, while both Rock-Eval 7S and the LECO SC-632 reach up to 1200 and 1350 °C, respectively (fully decomposing and detecting sulfur species). Also, the “trap and release” method in CHNS analyzers could be inefficient, resulting in lower yields.

### 3. RESULTS AND DISCUSSION

**3.1. Source-Rock Programmed Pyrolysis and OM Type.** Tables 1 and 2 summarize the Rock-Eval 7S pyrolysis and oxidation results for all 28 Bakken Shale samples (UBS and LBS) and the 5 additional outcrop samples included in this study. The 28 Bakken Shale samples were retrieved from 9 wells with varying levels of thermal maturity (from the margin to the center of the basin and along the Nesson Anticline). For thermally immature Bakken Shale samples ( $T_{\max}$  between 416 and 435 °C), the hydrogen index ( $HI = 100 \times S2/TOC$ ) values average 619 mg of HC/g of TOC for UBS samples and 632 mg of HC/g of TOC for LBS samples (Figure 5 and

Tables 1 and 2). These HI results show the variability expected for immature marine type II OM, such as the UBS and LBS.<sup>37–39</sup>

The HI values exponentially decrease (along with S2 values) with increasing thermal maturity, with HI values as low as 92–184 mg of HC/g of TOC ( $T_{\max}$  between 458 and 465 °C; see Tables 1 and 2). For the five thermally immature outcrop samples ( $T_{\max}$  values between 406 and 418 °C; 440 °C for the Green River sample), HI values vary from 697 to 960 mg of HC/g of TOC (Table 2). If we were to only use the classical guidelines for kerogen typing based on programmed pyrolysis results (as well as commonly used programmed pyrolysis plots),<sup>40–42</sup> four of the five outcrop samples (Green River Shale, Orbagnoux Carbonate, Pantokrator Shale, and Monterey Shale) can be classified as type I kerogens (HI between 764 and 960 mg of HC/g of TOC), while a fifth sample (the Kimmeridge Clay sample) can be classified as borderline type II (almost type I) marine kerogen. This can be seen in Table 2 and in the modified van Krevelen diagram in Figure 6A (OI versus HI, right plot).

Of the four samples clustering around the type I OM path in the modified van Krevelen diagram, only the Green River Shale is known to kinetically behave and generate the products expected of type I OM (i.e., does not enter the threshold for

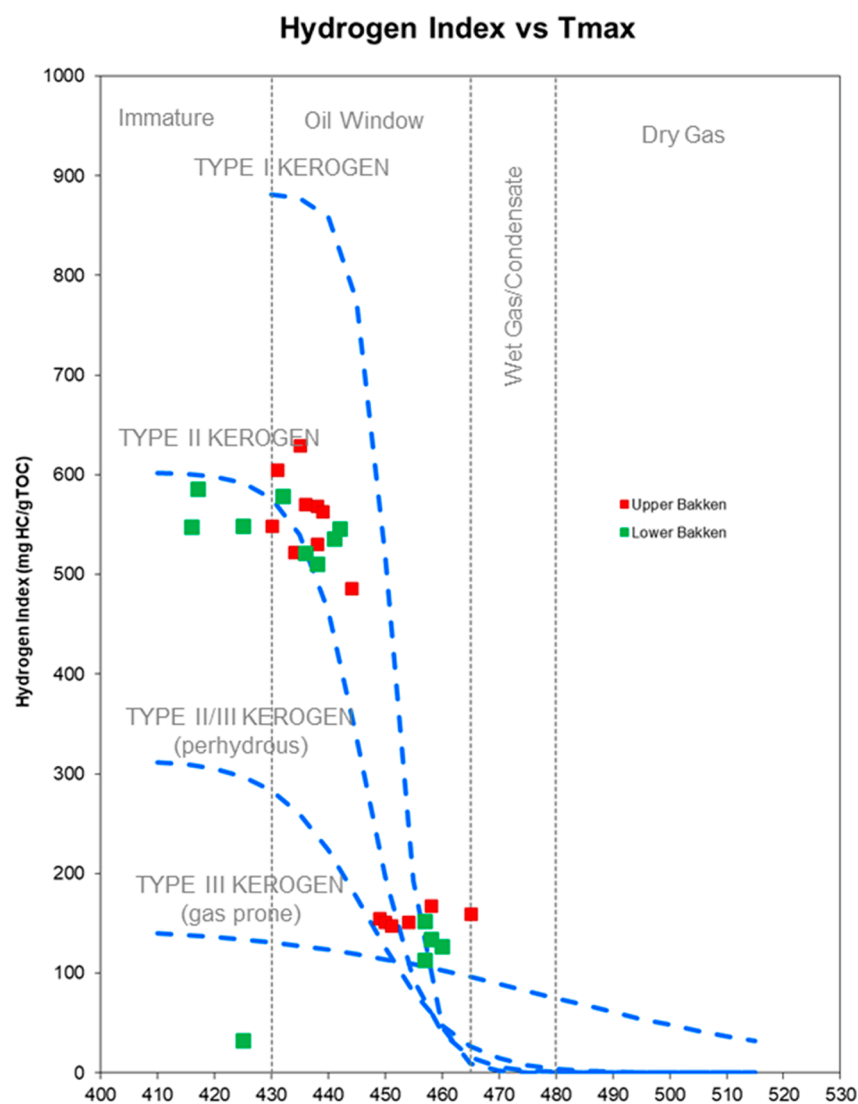


**Figure 5.** Programmed pyrolysis hydrogen index versus maturity diagram of the Bakken Shale samples. Bakken Shale samples plot along the type II OM trend.

hydrocarbon generation until  $T_{\max}$  of  $\sim 445$  °C). The remaining three samples are not composed of sedimentary OM type I. This has been a major pitfall of programmed pyrolysis interpretative plots (such as the modified van Krevelen diagram, right plot in Figure 6A) identified by many studies over the years.<sup>43,44</sup> This pitfall becomes problematic when the OM in the source rock of interest is rich in organic sulfur (type IS and type IIS kerogens), either in its entirety or by having organic facies that are rich in organic sulfur. Examples of both situations are the Monterey Shale<sup>7,9,11</sup> and sulfur-rich organic facies of the Eagle Ford Formation in Texas.<sup>1,13</sup>

Because plots such as the modified van Krevelen diagram or the popular cross-plot of TOC versus  $S_2$ <sup>45,46</sup> do not distinguish type II from type IIS or type I from type IS kerogens, many studies assume that high HI and low OI ( $\leq 17$ ) are indicative of type IIS kerogens.<sup>45</sup> However, this is not a very accurate way of performing kerogen typing of sulfur-rich kerogens. The most common practice for identification of source rocks with type IS and type IIS kerogens is through the determination of atomic ratios of sulfur/carbon ( $S_{\text{org}}/C$ ) and hydrogen/carbon (H/C). Mineral-free OM concentrates of

type II kerogens with atomic  $S_{\text{org}}/C$  ratios greater than 0.04 (or containing more than 8.0 wt % on a kerogen basis of organic sulfur) are classified as type IIS kerogens.<sup>7,11,45,46</sup> This method, however, involves intense wet chemistry separation of mineral fractions from the rock, as explained earlier.

The sulfur index ( $SI = \text{pyrolysis organic sulfur}/\text{TOC} \times 1000$ ), calculated routinely during Rock-Eval 7S pyrolysis and oxidation runs, is a fast, reliable, and cost-effective alternative to perform proper identification of type IIS and type IS kerogens.<sup>30,31,47</sup> The left diagram in Figure 6A cross-plots SI versus HI values and differentiates OM types in the same fashion that the atomic ratios  $S_{\text{org}}/C$  and H/C are cross-plotted for the identification of type IIS and type IS kerogens.<sup>48,49</sup> The cross-correlation of SI and HI accounts for the reactive organic sulfur (here referred to as  $S_{\text{org}}$ ) and readily separates type IS and type IIS from their sulfur-lean counterparts (i.e., type I and type II kerogens). Organic-rich rocks with SI of  $>100$  are classified as type IS or type IIS (depending upon their HI values).<sup>29,30,47</sup> A SI of  $\geq 100$  is equivalent to  $S_{\text{org}}/C = 0.04$  defined by Orr<sup>7</sup> as the lower limit for type IIS kerogens.<sup>29,30,47</sup> On the basis of the above, the four samples originally plotting around the type I path in the



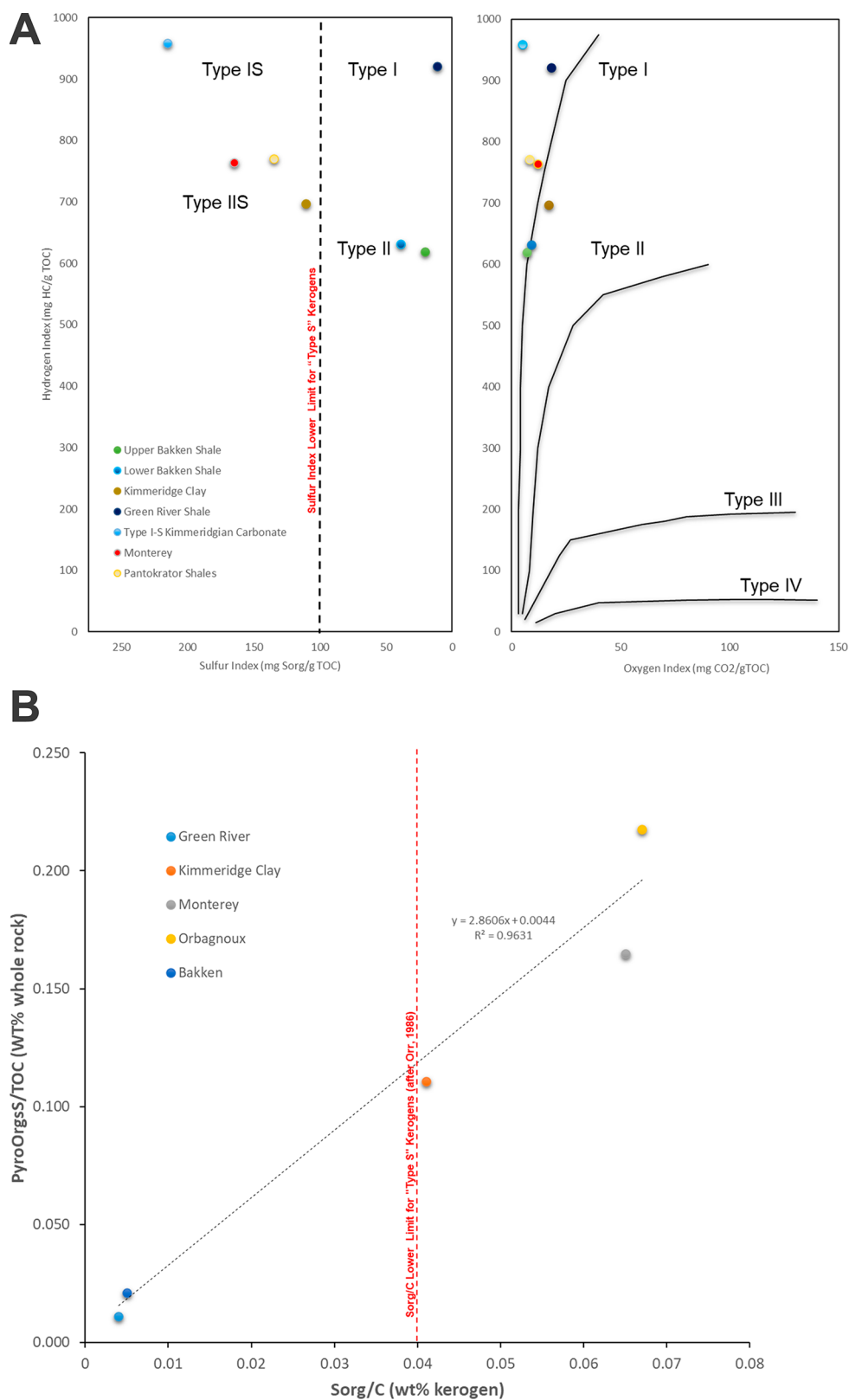


**Figure 6.** (A) Programmed pyrolysis interpretative plots for kerogen typing. The right plot shows the classic modified van Krevelen diagram separating the samples analyzed on the basis of their oxygen and hydrogen indices (OI versus HI). The left plot also separates the samples analyzed but based on their reactive, organic sulfur quantities (represented in the plot by the sulfur index; SI versus HI). See the text for more details. (B) Cross correlation of the atomic  $S_{org}/C$  ratio (from kerogen concentrates) versus the ratio of organic sulfur measured during Rock-Eval 7S pyrolysis/TOC (from whole rocks). Notice the excellent correlation between both indicators of type S kerogens and how the identification of type S OM derived from the SI in panel A stands.

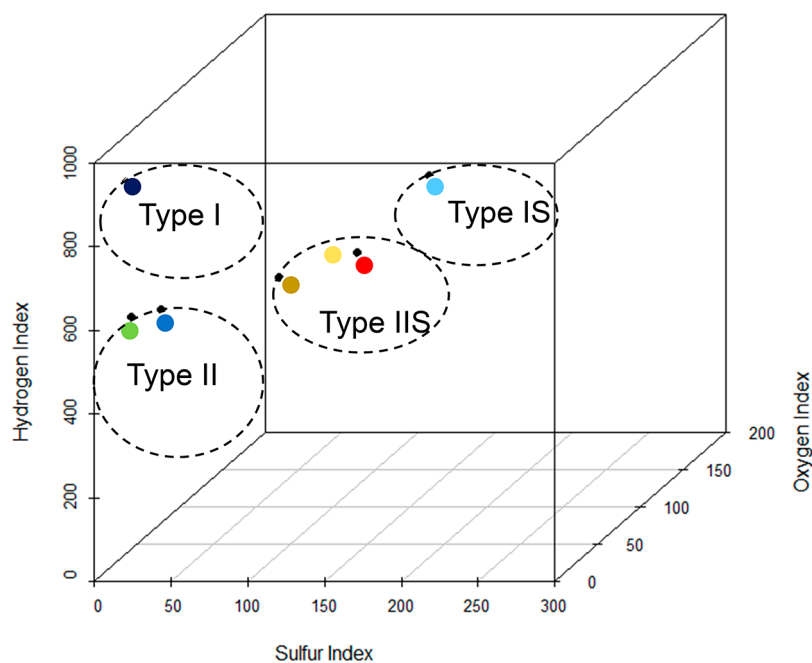


**Figure 7.** 3D plot of the three key parameters to differentiate kerogen types based on their sulfur, hydrogen, and oxygen contents. This type of plot shows a good separation of sulfur-rich versus sulfur-lean kerogen types by introducing the sulfur index. Sample colors are the same as in Figure 6.

modified van Krevelen diagram (right plot of Figure 6) are separated into type IIS (Kimmeridge Clay, Pantokrator Shale, and Monterey Shale) and type IS (Kimmeridgian Carbonate) by calculating their SI values using the sulfur differentiation parameters from the Rock-Eval 7S results (Table 2). The  $S_{\text{org}}/C$  ratios obtained for the Monterey Shale ( $S_{\text{org}}/C = 0.065$ ), Kimmeridge Clay ( $S_{\text{org}}/C = 0.042$ ), Orbagnoux Carbonate ( $S_{\text{org}}/C = 0.067$ ), and Green River Shale ( $S_{\text{org}}/C = 0.004$ ) samples as well as the average for the combined immature UBS and LBS samples ( $S_{\text{org}}/C = 0.005$ ) confirm the kerogen typing classification determined by the SI values and the SI versus HI cross-plot in Figure 6A. Furthermore, Figure 6B shows the excellent relationship between the  $S_{\text{org}}/C$  atomic ratio and the pyrolysis organic sulfur/TOC ratio (main term in the SI calculation). Notice also how the “type S” OM classifications from panels A and B of Figure 6 stand. The three-dimensional (3D) plot in Figure 7 includes the three kerogen typing parameters SI, HI, and OI and is a much better alternative to kerogen typing, because it clearly differentiates sulfur-rich (type IS and type IIS) from sulfur-lean (type I and type II) kerogens.

All of the Bakken Shale samples analyzed (both UBS and LBS) have SI values of  $<100$  (average  $SI_{\text{UBS}} = 20$  and  $SI_{\text{LBS}} = 27$ ; see Table 2) classifying them as type II marine OM, which confirms what has been known about the kinetic behavior of the UBS and LBS for the production of hydrocarbons.<sup>38,39,49</sup> Although the UBS and LBS members of the Bakken Shale are usually considered as type II marine, sulfur-lean kerogens, the reality is that both UBS and LBS, when immature and even after thermally maturing, contain significant amounts of organic sulfur (and, hence, high TOS values). This organic sulfur, however, is not associated with the reactive and labile portion of the TOC (i.e., S2-S) but with the refractory and usually considered “inert” portion of the TOC (S4 parameter from Rock-Eval analyses or residual carbon). This residual S can have a tremendous impact on the production of  $H_2S$  gas

upon thermal maturation<sup>18</sup> or during completions and enhanced oil recovery (EOR) phases.<sup>15,16</sup>

**3.2.  $H_2S$  Production from the Bakken Shale.** There are different forms of sulfur associated with the OM and mineral matrix in a rock, all with the potential to be chemically reactive as thermal maturity increases. Organic sulfur in sedimentary organic matter can be present in reduced or oxidized forms. Reduced forms are predominantly alkyl sulfides and aromatic forms (e.g., thiophenes, benzothiophenes, naphthalenes, and aryl disulfides), while the remainder of the organic sulfur pool is composed of oxidized species (e.g., sulfonates, sulfoxides, and sulfate esters).<sup>5,20</sup> The former is almost completely associated with pyrolyzable organic sulfur (i.e., S1-S and S2-S), while the latter is linked to the residual organic sulfur (ROS or S4-S) that is associated with the oxidized portion of the TOC (known as S4CO and S4CO<sub>2</sub>). This means that not all of the TOS found in sedimentary rocks is responsible for the early hydrocarbon generation kinetics seen in “type S” kerogens. Thus, high TOS values alone should not be considered as an indicator of the presence of type IIS and type IS kerogens. For proper identification of “type S” kerogens, the use of the SI values along with HI values is recommended (Figures 6 and 7).

However, high TOS in type II and type I kerogens (non-“type S” kerogens) can be an indication for potential gas souring (i.e.,  $H_2S$ ) upon kerogen cracking (as thermal maturity increases) and/or during EOR activities, as indicated by previous studies.<sup>15–18</sup> Souring of oil and gas production from the Bakken Shale in North Dakota and Montana has been a recognized issue in recent years.<sup>32,33</sup> Some studies have hypothesized that remineralization and decomposition of OM with increasing thermal maturity could potentially release sulfur as a source of thermogenic  $H_2S$ <sup>33</sup> in accordance to what has been hypothesized for the souring of oil and gas production within the Permian Basin.<sup>15–18</sup>

Notice from Table 2 that, although SI values in both UBS and LBS samples are well below those expected for “type S”

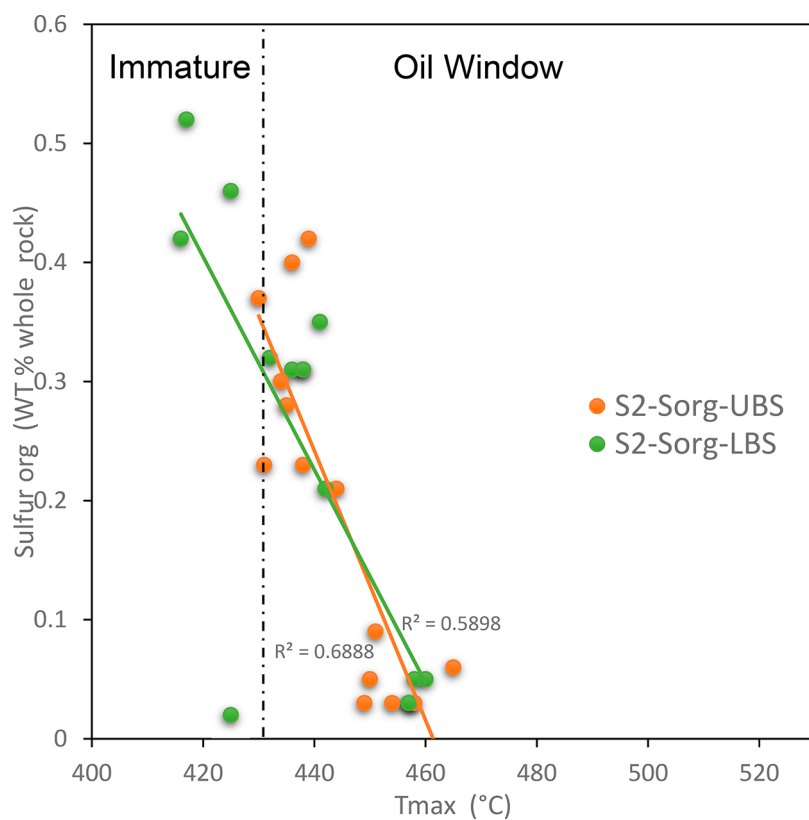


Figure 8. With an increasing maturity level, S2-S shows a general decrease in both UBS and LBS samples.

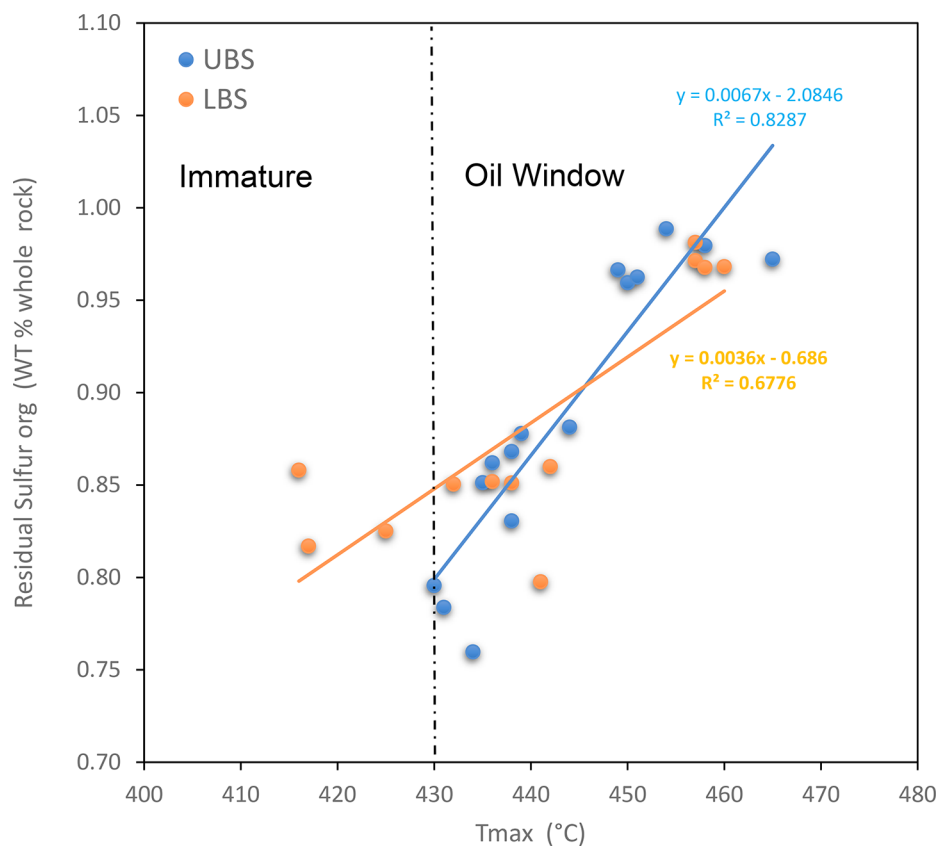
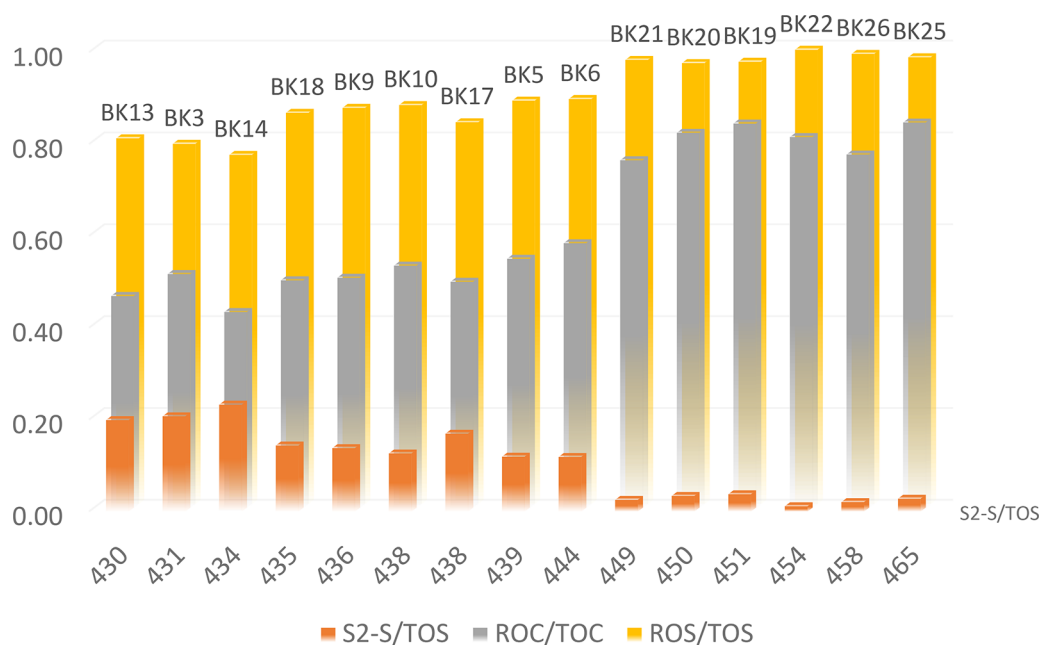
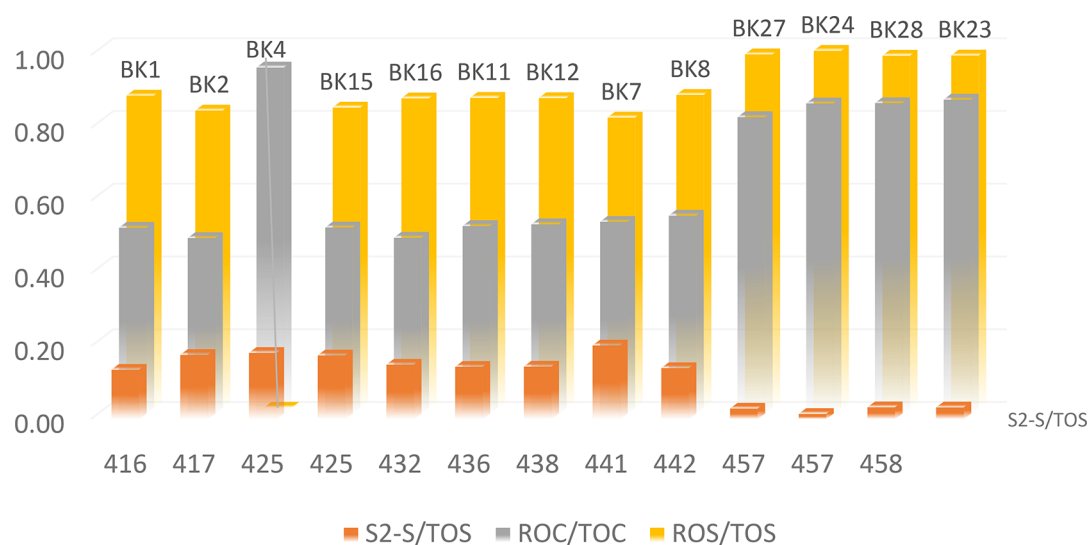


Figure 9. With an increasing maturity level, ROS shows a general increase in both UBS and LBS samples.



**Figure 10.** With an increasing maturity level, the ratio S2-S/TOS shows a general decrease in UBS samples, while the ratios ROC/TOC and ROS/TOS increase.



**Figure 11.** With an increasing maturity level, the ratio S2-S/TOS shows a general decrease in LBS samples, while the ratios ROC/TOC and ROS/TOS increase.

kerogens (i.e., SI of  $\geq 100$ ), the TOS values in UBS and LBS samples are similar to the “type S” kerogens (Monterey, Kimmeridge Clay, Pantokrator Shale, and type IS Orbagnoux Carbonate), with an average TOS = 2.0 wt %. Moreover, TOS values in the highly mature UBS and LBS samples are still high (e.g., samples BK22 and BK24 have TOS = 2.65 and 2.14 wt %, respectively, at  $T_{\max}$  between 454 and 457 °C). As noted by Xia and He,<sup>18</sup> to get to 10 vol % of H<sub>2</sub>S in a natural gas, one only need to thermally decompose a type II or type I kerogen with S = 1.4 wt % (or  $S_{\text{org}}/C = 0.005$ ), which is not even close to the amount of organic sulfur in “type S” kerogens. On the basis of the TOS values reported in Table 2, it seems that several samples from both UBS and LBS groups of samples can potentially be H<sub>2</sub>S producers if the right thermal stimulation (e.g., steam injection or similar EOR practices) was applied to their kerogen moieties. Figures 8–11 show a clearer picture of

what happens to the different organic sulfur fractions (reduced and oxidized) with increasing thermal maturity. As expected, the fraction of organic sulfur associated with labile kerogen (S2-S) is reduced as thermal maturity increases (Figures 8, 10, and 11). Conversely, the residual organic sulfur fraction associated with the S4 portion of the TOC (ROC in Figures 10 and 11) increases in parallel with thermal maturity (Figures 9–11). This leaves quite a lot of organic sulfur in the kerogen available for potential reactions, such as the aquathermolysis reaction described by Lamoureux-Var et al.<sup>15</sup> and the transformations described in Xie and He.<sup>17</sup> Of the 28 UBS and LBS samples, 10 samples came from wells where H<sub>2</sub>S issues have been reported. Well 12 with UBS samples BK13 and BK14 and LBS samples BK15 and BK16 have reported H<sub>2</sub>S values of 0.1%; well 14 with UBS samples BK18 and BK17 reported H<sub>2</sub>S values of 1.6 vol %; well 5 with UBS samples



BK5 and BK6 and LBS samples BK7 and BK8 reported H<sub>2</sub>S values of 0.1 vol %; and well 1 with LBS samples BK1 and BK2 reported H<sub>2</sub>S values of 7.3 vol %. The TOS values for these 10 samples average 2.13 wt % (on a whole-rock basis), which would equate to a much larger weight percent of sulfur than the minimum estimated by Xie and He<sup>17</sup> for H<sub>2</sub>S production (1.4 wt % S on a kerogen basis).

We emphasize the importance of understanding sulfur geochemistry in addressing safety and environmental concerns when designing hydrocarbon extraction strategies, such as hydraulic fracturing, from unconventional sulfur-rich formations. There are two major implications. First, these strategies may generate hazardous and toxic hydrogen sulfide gas (H<sub>2</sub>S) at concentrations of >100 ppm, as seen across the Greater Permian Basin in West Texas and New Mexico, U.S.A., where almost 85% of the gas in wells has a H<sub>2</sub>S content of >100 ppm and more than 40% have H<sub>2</sub>S of >10 000 ppm. Removing H<sub>2</sub>S from the gas streams has a high financial cost in field production. Second, organic sulfur-rich marine kerogen generates hydrocarbons at much lower maturity than sulfur-poor kerogen. This results in the onset to the oil window being encountered at shallower depths, which has a direct impact on drilling and completion costs.

#### 4. CONCLUSION

The following conclusions can be drawn: (1) The sulfur index (SI = pyrolysis organic sulfur/TOC × 1000), which is calculated during Rock-Eval 7S pyrolysis and oxidation runs, is a fast, reliable, and cost-effective alternative for the proper identification of type IIS and type IS kerogens. SI can replace time-consuming and labor-intensive wet chemistry methods. A SI value of 100 should be used to differentiate between kerogen type I versus type IS and type II versus type IIS more accurately compared to the widely used modified van Krevelen diagram of HI versus OI. (2) The Rock-Eval 7S TS results for a total of 28 Bakken Shale samples analyzed are in good agreement with the CHNS elemental analyzer results and in excellent agreement with the LECO SC-632 results. Minor discrepancies in yields observed are attributed to the fact that the elemental analyzer does not fully decompose sulfur species (especially sulfates) at 1000 °C, while Rock-Eval 7S and LECO SC-632 fully decompose sulfur species at 1200 and 1350 °C, respectively. (3) The 28 Upper and Lower Bakken samples contain significant amounts of organic sulfur, although their SI values are low (<100). However, the organic sulfur is not associated with the reactive and labile portion of the TOC (i.e., S2-S) but with the refractory or “inert” portion of the TOC or residual organic carbon (ROC). (4) High TOS values, by themselves, should not be considered as an indicator of the presence of type IIS and type IS kerogens in the samples. This is because not all of the TOS is responsible for the early hydrocarbon generation kinetics seen in “type S” kerogens. Thus, the use of the SI values, in association with HI values, is recommended for the proper identification of “type S” kerogens. (5) The TOS values in the Upper and Lower Bakken samples are similar to the “type S” kerogens in some of the other shales analyzed. Although the fraction of organic sulfur associated with labile kerogen (S2-S) in the Bakken Shale is reduced as thermal maturity increases, the residual organic sulfur fraction associated with the S4 portion of the TOC increases in the same direction. This means that a considerable amount of organic sulfur in the Bakken kerogen is available to generate H<sub>2</sub>S by aquathermolysis reactions. This

process has also been proposed to explain the high H<sub>2</sub>S production seen in wells from the Greater Permian Basin in Texas and New Mexico. (6) Bakken samples having high TOS can potentially be H<sub>2</sub>S producers in the Williston Basin if the right thermal stimulation (e.g., steam injection or similar EOR practices) were to be applied to their kerogen moieties. The TOS values for 10 of the 28 samples average 2.13 wt % (on a whole-rock basis), which is a considerably larger weight percent of sulfur than the minimum amount estimated for H<sub>2</sub>S production (1.4 wt % S on a kerogen basis). These 10 Bakken samples came from wells that have seen high H<sub>2</sub>S production, thus suggesting a possible relationship between TOS and H<sub>2</sub>S.

#### ■ AUTHOR INFORMATION

##### Corresponding Author

Thomas Gentzis – Reservoir Geology, Core Laboratories, Houston, Texas 77040, United States; [orcid.org/0000-0003-4592-9318](https://orcid.org/0000-0003-4592-9318); Email: [thomas.gentzis@corelab.com](mailto:thomas.gentzis@corelab.com)

##### Authors

Humberto Carvajal-Ortiz – Reservoir Geology, Core Laboratories, Houston, Texas 77040, United States

Mehdi Ostadhassan – Key Laboratory of Continental Shale Hydrocarbon Accumulation and Efficient Development, Ministry of Education, Northeast Petroleum University, Daqing, Heilongjiang 163318, People's Republic of China; [orcid.org/0000-0001-9235-4399](https://orcid.org/0000-0001-9235-4399)

Complete contact information is available at:

<https://pubs.acs.org/10.1021/acs.energyfuels.1c01562>

##### Notes

The authors declare no competing financial interest.

#### ■ ACKNOWLEDGMENTS

The authors thank the Core Library, North Dakota Geological Survey, for granting access to the Bakken core samples, particularly Jeffrey Bader, state geologist and director, as well as Kent Hollands, lab technician. The authors also appreciate the assistance provided by Bailey Bubach of the University of North Dakota, for collecting and plotting the SO<sub>4</sub> data in Figure 1. Professor Francois Baudin, Sorbonne University in France, reviewed an earlier draft of the manuscript and provided valuable comments. Stacy McWhorter, General Manager of Integrated Reservoir Solutions & US Geosciences, Core Laboratories, Houston, TX, and Ken Mosley, Manager of Geology, Core Laboratories, Houston, TX, are thanked for their continuous support and encouragement. Finally, the authors express their gratitude to the two reviewers for their time and effort to review the manuscript and Professor Praveen Linga for his professional handling of the manuscript through the review process.

#### ■ REFERENCES

- (1) Tissot, B. P.; Welte, D. H. *Petroleum Formation and Occurrence*; Springer-Verlag: Berlin, Germany, 1984.
- (2) Curiale, J. A.; Curtis, J. B. Organic geochemical applications to the exploration for source-rock reservoirs—A review. *J. Unconv. Oil Gas Resour.* **2016**, *13*, 1–31.
- (3) Eglinton, T. I.; Sinninghe Damsté, J. S.; Kohnen, M. E. L.; de Leeuw, J. W.; Larter, S. R.; Patience, R. L. Analysis of maturity-related changes in organic sulfur composition of kerogens by flash pyrolysis—gas chromatography. In *Geochemistry of Sulfur in Fossil Fuels*; Orr, W. L., White, C. M., Eds.; American Chemical Society (ACS):

Washington, D.C., 1990; ACS Symposium Series, Vol. 429, Chapter 27, pp 529–565, DOI: 10.1021/bk-1990-0429.ch027.

(4) Boussafir, M.; Lallier-Vergès, E. Accumulation of organic matter in the Kimmeridge Clay Formation (KCF), an update fossilisation model for marine petroleum source-rocks. *Mar. Pet. Geol.* **1997**, *14*, 75–83.

(5) Raven, M. R.; Fike, D. A.; Gomes, M. L.; Webb, S. M.; Bradley, A. S.; McClelland, H.-L.O. Organic carbon burial during OAE2 driven by changes in the locus of organic matter sulfurization. *Nat. Commun.* **2018**, *9*, 3409.

(6) Lewan, M. Sulphur-radical control on petroleum formation rates. *Nature* **1998**, *391*, 164–166.

(7) Orr, W. L. Kerogen/asphaltene/sulfur relationships in sulfur-rich Monterey oils. *Org. Geochem.* **1986**, *10*, 499–516.

(8) Orr, W. L. Evaluating kerogen sulfur content from crude oil properties: Cooperative Monterey Organic Geochemistry Study. In *The Monterey Formation: From Rocks to Molecules*; Isaacs, C. M., Rullkötter, J., Eds.; Columbia University Press: New York, 2001; pp 348–367.

(9) Baskin, D. K.; Peters, K. E. Early generation characteristics of a sulfur-rich Monterey kerogen. *AAPG Bull.* **1992**, *76*, 1–13.

(10) Orr, W. L.; Sinninghe Damsté, J. S. Geochemistry of Sulfur in Petroleum Systems. In *Geochemistry of Sulfur in Fossil Fuels*; Orr, W. L., White, C. M., Eds.; American Chemical Society (ACS): Washington, D.C., 1990; ACS Symposium Series, Vol. 429, Chapter 1, pp 2–29, DOI: 10.1021/bk-1990-0429.ch001.

(11) Jarvie, D. E.; Lundell, L. L. Kerogen type and thermal transformation of organic matter in the Miocene Monterey Formation. In *The Monterey Formation: From Rocks to Molecules*; Isaacs, C. M., Rullkötter, J., Eds.; Columbia University Press: New York, 2001; Chapter 15, pp 268–295.

(12) Little, J.; Formolo, M. J.; Lewan, M. D. Correlating Oils in Turonian–Cenomanian Source Rocks Using Hydrous Pyrolysis and Organic Sulfur Compounds. *Proceedings of the AAPG Annual Convention and Exhibition*; Long Beach, CA, April 22–25, 2012; Article 10453.

(13) Lillis, P. G. Application of Oil Gravity and Sulfur Content Relationships to Oil Typing and Source Rock Kinetics. *Proceedings of the 2017 AAPG National Meeting*; Houston, TX, April 2–5, 2017; Article 42174.

(14) French, K. L.; Birdwell, J. E.; Lewan, M. D. Trends in thermal maturity indicators for the organic sulfur-rich Eagle Ford Shale. *Mar. Pet. Geol.* **2020**, *118*, 104459.

(15) Lamoureux-Var, V.; Ouled Ameer, Z.; Michel, P.; Lévêque, I.; Ravin, A.; Pillot, D.; Ayache, S.; Preux, C. Characterizing Sulfur in Foster Creek Bitumen Using Rock-Eval Sulfur, for Assessing H<sub>2</sub>S Production Risk in SAGD Operations. *Proceedings of the First EAGE/IPPEN Conference on Sulfur Risk Management in E&P*; Rueil-Malmaison, France, Sept 18–20, 2018.

(16) Lamoureux-Var, V.; Lorant, F. Experimental evaluation of H<sub>2</sub>S yields in reservoir rocks submitted to steam injection. *Proceedings of the IOR 2005–13th European Symposium on Improved Oil Recovery*; Budapest, Hungary, April 25–27, 2005.

(17) Xia, X.; Ellis, G. S. Coupled Kinetic and Fluid Dynamic Models to Understand H<sub>2</sub>S Occurrence in Unconventional Petroleum Reservoirs. *Proceedings of the SPE/AAPG/SEG Unconventional Resources Technology Conference*; San Antonio, TX, Aug 1–3, 2016; Paper URTEC-2460230-MS, DOI: 10.15530/urtec-2016-2460230.

(18) Xia, D.; He, Z. Hydrogen Sulfide (H<sub>2</sub>S) in the Permian Basin. *Proceedings of the AAPG 2017 Annual Convention and Exhibition*; Houston, TX, April 2–5, 2017; Article 10950.

(19) Pomerantz, A. E.; Bake, K. D.; Craddock, P. R.; Kurzenhauser, K. W.; Kodalen, B. G.; Mitra-Kirtley, S.; Bolin, T. B. Sulfur speciation in kerogen and bitumen from gas and oil shales. *Org. Geochem.* **2014**, *68*, 5–12.

(20) Bolin, T. B.; Birdwell, J. E.; Lewan, M. D.; Hill, R. J.; Grayson, M. B.; Mitra-Kirtley, S.; Bake, K. D.; Craddock, P. R.; Abdallah, W.; Pomerantz, A. E. Sulfur species in source rock bitumen before and

after hydrous pyrolysis determined by X-ray absorption near-edge structure. *Energy Fuels* **2016**, *30*, 6264–6270.

(21) Spiro, C. L.; Wong, J.; Lytle, F. W.; Gregor, R. B.; Maylotte, D. H.; Lamson, S. H. X-ray absorption spectroscopic investigation of sulfur sites in coal: Organic sulfur identification. *Science* **1984**, *226*, 48–50.

(22) George, G. N.; Gorbaty, M. L. Sulfur K-edge X-ray absorption spectroscopy of petroleum asphaltenes and model compounds. *J. Am. Chem. Soc.* **1989**, *111*, 3182–3186.

(23) Huffman, G. P.; Mitra, S.; Huggins, F. E.; Shah, N.; Vaidya, S.; Lu, F. Quantitative analysis of all major form of sulfur in coal by X-ray absorption fine structure spectroscopy. *Energy Fuels* **1991**, *5*, 574–581.

(24) Wiltfong, R.; Mitra-Kirtley, S.; Mullins, O. C.; Andrews, B.; Fujisawa, G.; Larsen, J. W. Sulfur speciation in different kerogens by XANES spectroscopy. *Energy Fuels* **2005**, *19*, 1971–1976.

(25) Kelemen, S. R.; Afeworki, M.; Gorbaty, M. L.; Sansone, M.; Kwiatek, P. J.; Walters, C. C.; Freund, H.; Siskin, M.; Bence, A. E.; Curry, D. J.; Solum, M.; Pugmire, R. J.; Vandenbroucke, M.; Leblond, M.; Behar, F. Direct characterization of kerogen by X-ray and solid-state <sup>13</sup>C nuclear magnetic resonance methods. *Energy Fuels* **2007**, *21*, 1548–1561.

(26) Kelemen, S. R.; Walters, C. C.; Kwiatek, P. J.; Freund, H.; Afeworki, M.; Sansone, M.; Lamberti, W. A.; Pottorf, R. J.; Machel, H. G.; Peters, K. E.; Bolin, T. Characterization of solid bitumens originating from thermal chemical alteration and thermochemical sulfate reduction. *Geochim. Cosmochim. Acta* **2010**, *74*, 5305–5332.

(27) Frank, P.; Hedman, B.; Carlson, R. M. K.; Tyson, T. A.; Roe, A.; Hodgson, K. O. A large reservoir of sulfate and sulfonate resides within plasma cells from *Ascidia ceratodes*, revealed by X-ray absorption near-edge structure spectroscopy. *Biochemistry* **1987**, *26*, 4975–4979.

(28) Madec, M.; Espitalié, J. Determination of organic sulphur in sedimentary rocks by pyrolysis. *J. Anal. Appl. Pyrolysis* **1985**, *8*, 201–219.

(29) Wattripont, A.; Bouton, N.; Espitalié, J.; Antonas, R. Rock-Eval Sulfur & GEOWORKS software. *Proceedings of the First EAGE/IPPEN Conference on Sulfur Risk Management in Exploration and Production*; Rueil-Malmaison, France, Sept 18–20, 2018; DOI: 10.3997/2214-4609.201802756.

(30) Aboussou, A.; Lamoureux-Var, V.; Wagner, T.; Pillot, D.; Kowalewski, I.; März, C.; Garcia, B.; Doligez, B. Pyritic Sulphur and Organic Sulphur Quantification in Organic Rich Sediments Using Rock-Eval. *Proceedings of the First EAGE/IPPEN Conference on Sulfur Risk Management in Exploration and Production*; Rueil-Malmaison, France, Sept 18–20, 2018; DOI: 10.3997/2214-4609.201802758.

(31) Aboussou, A.; Lamoureux-Var, V.; Wagner, T.; Pillot, D.; Kowalewski, I.; März, C.; Garcia, B.; Doligez, B. Application of an Advanced Method for Pyritic and Organic Sulphur Quantification to Organic Rich Marine Sediments. *Proceedings of the 80th EAGE Conference and Exhibition 2018*; Copenhagen, Denmark, June 11–14, 2018; DOI: 10.3997/2214-4609.201801129.

(32) Holubnyak, Y. I.; Breme, J. M.; Mibeck, B.; Hambling, J. A.; Huffman, B. J.; Klapperich, R. J.; Smith, S. A.; Sorensen, J. A.; Harju, J. A. Understanding the souring at Bakken oil reservoirs. *Proceedings of the SPE International Symposium on Oilfield Chemistry*; Woodlands, TX, April 11–13, 2011; Paper SPE-141434-MS, DOI: 10.2118/141434-MS.

(33) Abarghani, A.; Gentzis, T.; Liu, B.; Khatibi, S.; Bubach, B.; Ostadhassan, M. Preliminary Investigation of the effects of thermal maturity on redox-sensitive trace metal concentration in the Bakken source rock, North Dakota, USA. *ACS Omega* **2020**, *5*, 7135–7148.

(34) Behar, F.; Beaumont, V.; De B. Penteado, H. L. Rock-Eval 6 technology: Performances and developments. *Oil Gas Sci. Technol.* **2001**, *56*, 111–134.

(35) Fadeeva, V. P.; Tikhova, V. D.; Nikulicheva, O. N. Elemental analysis of organic compounds with the use of automated CHNS analyzers. *J. Anal. Chem.* **2008**, *63*, 1094–1106.

- (36) ThermoFisher Scientific. *FlashSmart Elemental Analyzer*; <https://www.thermofisher.com/order/catalog/product/11206100> (accessed June 1, 2019).
- (37) Baskin, D. K. Atomic H/C ratio of kerogen as an estimate of thermal maturity and organic matter conversion. *AAPG Bull.* **1997**, *81*, 1437–1450.
- (38) Jin, H.; Sonnenberg, S. A. Characterization for source rock potential of the Bakken Shales in the Williston Basin, North Dakota and Montana. *Am. Assoc Petrol Geol.* **2013**, 117–126.
- (39) Abarghani, A.; Ostadhassan, M.; Gentzis, T.; Carvajal-Ortiz, H.; Bubach, B. Organofacies study of the Bakken source rock in North Dakota, USA, based on organic petrology and geochemistry. *Int. J. Coal Geol.* **2018**, *188*, 79–93.
- (40) Peters, K. E. Guidelines for evaluating petroleum source rock using programmed pyrolysis. *AAPG Bull.* **1986**, *70*, 318–329.
- (41) Peters, K. E.; Cassa, M. R. Applied source rock geochemistry. In *The Petroleum System—From Source to Trap*; Magoon, L. B., Dow, W. G., Eds.; American Association of Petroleum Geologists: Tulsa, OK, 1994; pp 93–120, DOI: 10.1306/m60585c5.
- (42) Hart, B.; Steen, A. S. Programmed pyrolysis (Rock-Eval) data and shale paleoenvironmental analyses: A review. *Interpretation* **2015**, *3*, SH41–SH58.
- (43) Dembicki, H., Jr. Three common source rock evaluation errors made by geologists during prospect or play appraisals. *AAPG Bull.* **2009**, *93*, 341–356.
- (44) Dembicki, H., Jr. *Practical Petroleum Geochemistry for Exploration and Production*; Elsevier: Amsterdam, Netherlands, 2017; pp 751.
- (45) Langford, F. F.; Blanc-Valleron, M.-M. interpreting Rock-Eval pyrolysis data using graphs of pyrolizable hydrocarbons vs. total organic carbon. *AAPG Bull.* **1990**, *74*, 799–804.
- (46) Cornford, C. *Source Rocks and Hydrocarbons of the North Sea*; Glennie, K. W., Ed.; Wiley: Hoboken, NJ, 1998; Chapter 11, DOI: 10.1002/9781444313413.ch11.
- (47) Espitalié, J. Personal communication, 2020.
- (48) Huc, A. Y. *Geochemistry of Fossil Fuels: From Conventional to Unconventional Hydrocarbon Systems*; Editions Technips: Paris, France, 2013; ISBN: 978-2-7108-0990-6.
- (49) Baudin, F.; Tribouillard, N.; Trichet, J. *Géologie de la Matière Organique (Geospheres)*, 2nd ed.; EDP Sciences: Paris, France, 2017.